STATE RESEARCH CENTER OF RUSSIA

INSTITUTE FOR HIGH ENERGY PHYSICS

Addendum

to the Task C of the Accord between FNAL and IHEP

A.Abramov, I.Azhgirey, P.Galkin, N.Galyaev, V.Garkusha, A.Kharlamov, I.Kurochkin, E.Lomakin, F.Novoskoltsev, A.Ryabov, V.Zapolsky, V.Zarucheisky

Protvino 1998

Contents

1 Full Scale Target

Distributions of the energy deposition density in target teeth, as well as that of thermal stresses are in strong dependence on transversal distributions of the proton beam. This Addendum verifies design parameters of the full scale fin target described in the Task C IHEP Report [1] taking into account distributions of the proton beam obtained from more detail simulations of the MI extracting system.

The phase space distribution of the proton beam (x,x',y,y',p; total number of particles is equal to 100000) [2] at the input of the electrostatic septum was used by TURTLE code for simulation of beam parameters in the target. Strengths at last five quadrupoles (Q6÷Q10) of the proton beamline optics [3] were calculated using TRANSPORT code in order to obtain needed proton beam spot size. Energy deposition, temperature and stress calculations have been carried out for the baseline intensity equal to $4{\cdot}10^{13}$ protons/spill, as well as for $6{\cdot}10^{13}$ protons/spill. The maximum value of the beam size on the target was limited by the value of $\sigma = 2$ mm, taking into account values of inner radii for horns and baffle collimators.

1.1 Stresses in the Target. Length of the Target Tooth

The analysis of results obtained by a Monte Carlo simulation of the proton beam transport to the NuMI target using mentioned above input conditions shows that:

- the proton beam is essentially non-symmetrical in the horizontal plane (X–direction);
- the beam distribution in the vertical plane (Y–direction) is symmetrical, but non–Gaussian and may be described well by the 8-th order polynomial $N(y) = \sum_{k=0}^{4} \alpha_k \cdot y^{2k}$.

Results of stress calculations in the target as functions of the tooth length are shown in Figure 1.1 for graphite target and in Figure 1.2 for beryllium one. As it follows from these Figures:

- for graphite target the equivalent stress reaches its minimum value of 16.3 MPa at the length of the tooth equal to 6.2 mm;
- for beryllium target the equivalent stress reaches its minimum value of 117 MPa at the length of the tooth equal to 8 mm.

For these values of tooth lengths and taking into account the length of the gap between target teeth (at least 2 mm) and rounding of teeth corners, the longitudinal structure of both graphite and beryllium fin targets will considerably differ from that described in [1]. In this case the target will consists of 12–14 segments with small gaps between them.

Using the same longitudinal structure of the full scale target, as it is described in [1], stresses will increase by the factor of 1.46 from 16.3 MPa up to 23.8 MPa ($L_t = 18.4$ mm) for the graphite target and of 1.07 from 117 MPa up to 125 MPa ($L_t = 12.6$ mm) for the beryllium one.

It is necessary to note that asymmetry of the beam in the horizontal plane leads to the asymmetry of stresses on the lateral sides of the target in a case of vertical location of the target fin. This asymmetry of stresses reaches the value of (17–20) MPa for the beryllium target. In order to symmetrize stresses at the lateral sides of the target and to decrease their values it is more reasonable to locate the target fin in the horizontal plane. Contrary to the vertical location of the target fin where $\sigma_{\rm y} \simeq 2\sigma_{\rm x}$, in this case the beam should be stretched in horizontal plane ($\sigma_{\rm x} \simeq 2\sigma_{\rm y}$) in order to keep the same density of the energy deposition. But it may lead to the additional instability of the proton beam in the target in the horizontal plane and it should be also studied for such target fin location.

1.2 Targets for the Intensity of $6 \cdot 10^{13}$ protons/spill

1.2.1 Graphite Target

Since proton beam sizes for the baseline graphite target (with the beam intensity of $4 \cdot 10^{13}$ p/spill) is equal to $\sigma_{\rm x} = 0.71$ mm and $\sigma_{\rm y} = 1.44$ mm, decreasing of the energy deposition density can be achieved by increasing of $\sigma_{\rm y}$ up to limit value equal to 2.0 mm. Stresses in the graphite target for $\sigma_{\rm x} = 0.71$ mm and $\sigma_{\rm y} = 2.0$ mm for the beam intensity $6 \cdot 10^{13}$ p/spill are shown in Figure 1.3.

As one can see, for the tooth length equal to 18.4 mm [1] the equivalent stress is equal to 27.7 MPa and reaches its minimum value of 20.4 MPa for the tooth length $L_t = 7.8$ mm. At this value of L_t the stress in the baseline graphite target ($4 \cdot 10^{13}$ p/spill, $\sigma_{\rm y} \simeq 2\sigma_{\rm x}$) will be equal to 19.4 MPa (see Figure 1.1). Thus the graphite target with thickness of 3.2 mm and the tooth length of 7–8 mm may be used for proton beam intensities of

$(4\text{–}6)\cdot 10^{13}$ p/spill. Calculations of neutrino flux show that for such graphite target the increase of the primary proton beam intensity in 1.5 times gives practically the same increase of the total neutrino event rate at the far detector.

1.2.2 Beryllium Target

If the beam spot size is limited by the value of $\sigma = 2$ mm, then the baseline beryllium target with the thickness of 4.1 mm ($\sigma_x \simeq 1$ mm, $\sigma_y \simeq 2$ mm) could not be used for the proton beam intensity of $6\cdot 10^{13}$ p/spill because of stresses increase approximately by the factor of 1.5. Thus increasing of the target thickness is the only way for the beryllium target for this intensity. As calculations show, to obtain acceptable values of stresses, the thickness of the target fin should not be less than 5.5 mm.

Stresses in the beryllium target with the thickness of 5.5 mm as functions of the length of the tooth for the beam intensity of $6\cdot 10^{13}$ p/spill are shown in Figure 1.4. The minimum equivalent stress is equal to 140 MPa at the tooth length of 8.0 mm. This value of the equivalent stress corresponds to the safety factor equal to 1.7.

As it follows from Figure 1.2, the optimum length of the tooth for the baseline target is equal to 8 mm (117 MPa) and the longitudinal structure of the target may be the same for both proton beam intensities. Due to extra absorption of secondaries in the target fin with larger thickness, the total neutrino event rate at the far detector for the proton beam intensity $6\cdot 10^{13}$ p/spill is only 1.4 times higher than that for the the baseline intensity of $4\cdot 10^{13}$ p/spill.

1.3 Proton Beam Parameters in Targets

Parameters of proton beam in graphite and beryllium targets and corresponding values of strengths for last five quadrupoles Q6$\div$Q10 of the proton beamline are given in Table 1.1.

Beam parameters	$4{\cdot}10^{13}$ p/spill		$6{\cdot}10^{13}$ p/spill	
	Graphite	Beryllium	Graphite	Beryllium
$\sigma_{\rm x}$, mm	0.71	1.03	0.71	1.45
$\sigma_{\rm y}$, mm	1.44	2.02	2.00	1.96
$D_{\rm x}$, mm/%	16.25	0.	14.77	0.
$D_{\rm y}$, mm/%	0.	5.87	0.	22.10
Magnet	Strength, kG/m			
Q6	57.5622	57.9890	61.5140	56.5475
Q7	-63.4403	-68.1282	-70.8751	-64.7196
Q8	-84.3250	-76.2531	-83.2448	-71.0379
Q9	97.7019	81.9936	94.7428	76.2976
Q10	-18.1681	-8.6077	-9.1873	-12.0203

Table 1.1: Proton beam parameters and strengths of Q6÷Q10 quadrupoles.

2 Target Prototypes

After the Task C Report had been completed, following calculations and measurements were carried out for target prototypes design:

- calculations of stresses in the prototype of the graphite target as a function of rounding radius;
- calculations of dynamic stresses in the graphite prototype;
- measurements of thermoresistance between base, pressing plates and the target piece.

2.1 Stress Calculations

Stresses in the graphite target prototype have been computed by ANSYS using the energy deposition density from MARS calculations.

2.1.1 Stresses as Function of the Rounding Radius

Calculations of stresses in the target tooth as a function of rounding radius were made for the prototype of the graphite target under the testing intensity of $1{\cdot}10^{13}$ p/spill. Results of these calculations are given in Figure 2.1 in terms of the ratio of maximum equivalent stress at rounded surface to the equivalent stress at the point ($x = +d/2$, $y = 0$, $z = L_t/2$). As it follows from this plot, rounding of the corner does not avoid the stress concentration completely. Even for maximum rounding radius equal to a half of fin thickness, its value is equal to 13%. This increasing of the stress should be taking into account in calculations of the safety factor of the target.

2.1.2 Dynamic Stresses in the Graphite Target

In order to calculate dynamic stresses caused by fast extracted proton beam in the graphite prototype the 3D non–stationary problem of the target tooth without rounding of target corners has been solved by ANSYS for testing intensity equal to $1{\cdot}10^{13}$ p/spill. The length of the tooth was taken 6.5 mm, pulse duration was equal to 10 μs.

The thin structure of stresses varying in time at the point corresponding to the center of the target tooth (0,0,0) is shown in Figure 2.2. The time momentum 10 μs corresponds to the end of the proton beam spill. Periods of stresses oscillations reflect well the target tooth sizes: $S_{\rm xx}$ oscillations correspond to the sound wave length equal to the double tooth thickness, $S_{\rm yy}$ – to the double tooth height and $S_{\rm zz}$ – to the double tooth length. $S_{\rm zz}$ has maximum amplitude of oscillations and defines the amplitude of oscillations of $S_{\rm eq}$. But the amplitude of oscillation is equal to ∼0.3 MPa, i.e. only 1% from the value of quasi–static thermal stress. Similar curves were obtained for stresses in points 2 $(+d/2,0,0)$ and 3 $(0,0,L_t/2)$. The amplitude of stress oscillations at these points does not exceed of 1% from quasi–static thermal stress too.

2.2 Measurements of the Efficiency of the Water Cooling System

The efficiency of the water cooling system of target prototypes was verified by measuring of difference in temperature rise between pressing (base) plates and the target piece caused by heated water circulating through the cooling system.

The temperature of the base plate, as well as of the target tooth were monitored by means of J–type thermocouples similar to those used for the nickel–pad beam position indicator. The thermo-e.m.f. of thermocouples were measured by two Solartron 7065 microprocessor voltmeters. The water temperature was stabilized by Colora Ultra–Thermostat. In order to avoid the error due to the discrepancy between thermocouple curves (Voltage–

temperature), temperatures of the base plate, as well as of the target tooth were measured by both thermocouples inverting their positions. The amplitude of e.m.f. were $\sim$700 μV with voltmeter sensitivity equal to 1 μV.

In order to estimate the thermoresistance between the base (pressing) plate and the target piece the temperature of the target tooth in the point corresponding to the proton beam location was measured too. Measurements show, that:

- the ratio of the target tooth temperature rise at the point $\sim$(2–3) mm aside from the end of the base plate to the temperature rise of the base plate itself was equal to 1 ± 0.02;
- the temperature of the target tooth at the point of the proton beam location was lower than the temperature of the base plate in 150 μV.

Taking into account the maximum difference in temperature of the base plate and the target tooth equal to $700 \cdot 2 \cdot 10^{-2} = 14\,\mu$V, one may estimate the relative temperature jump at the thermoresistance between the base (pressing) plate and the target piece as $14\,\mu\text{V}/150\,\mu\text{V} \simeq 0.1$.

References

[1] Advanced Conceptual Design of the Full Scale Fin Target and Engineering Design of the Target Prototypes for the NuMI Project, Protvino, 1998.

[2] John Johnstone, Private communication.

[3] Status Report: Technical Design of Neutrino Beams for the Main Injector (NuMI), FNAL-TM-1946, NuMI-B-92, Batavia, 1995.

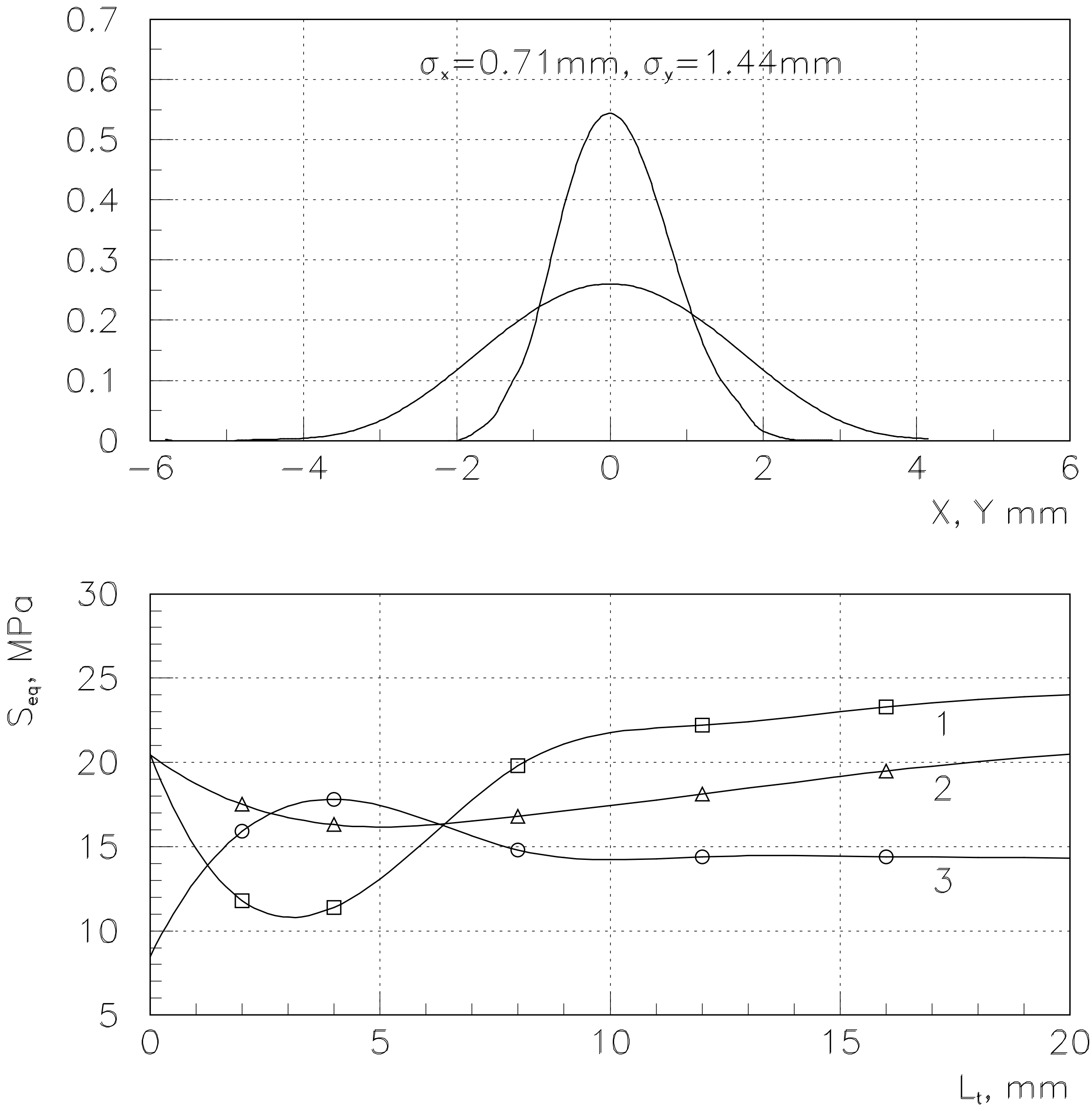

Figure 1.1: Normalized transversal beam distributions in the graphite target and equivalent stresses in most critical points as functions of the tooth length: 1 – point (0,0,0); 2 – point $(+d/2,0,0)$; 3 – point $(0,0,\pm L_t/2)$. Beam intensity is equal to $4{\cdot}10^{13}$ p/spill.

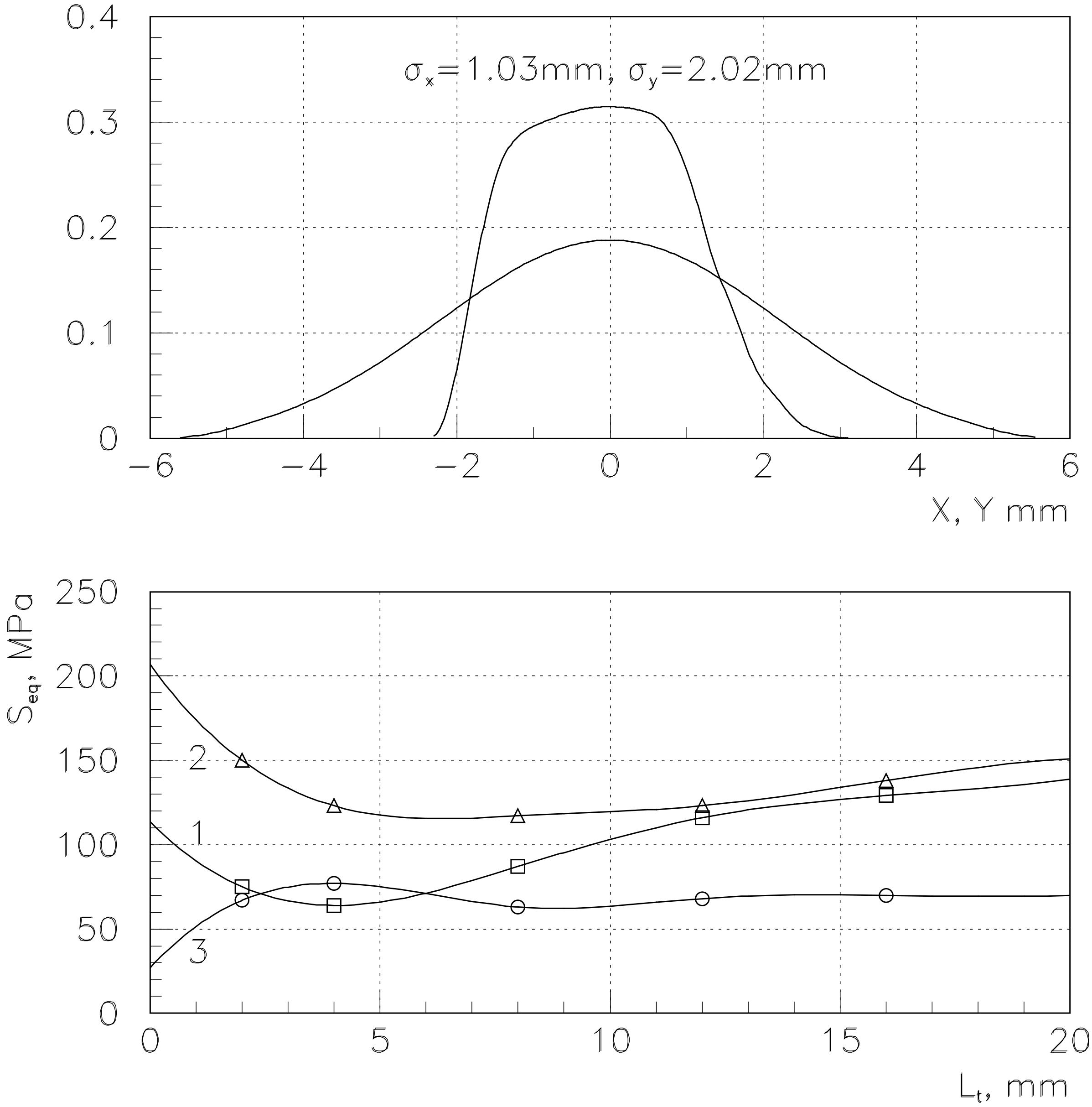

Figure 1.2: Normalized transversal beam distributions in the beryllium target and equivalent stresses in most critical points as functions of the tooth length: 1 – point (0,0,0); 2 – point $(+d/2,0,0)$; 3 – point $(0,0,\pm L_t/2)$. Beam intensity is equal to $4{\cdot}10^{13}$ p/spill.

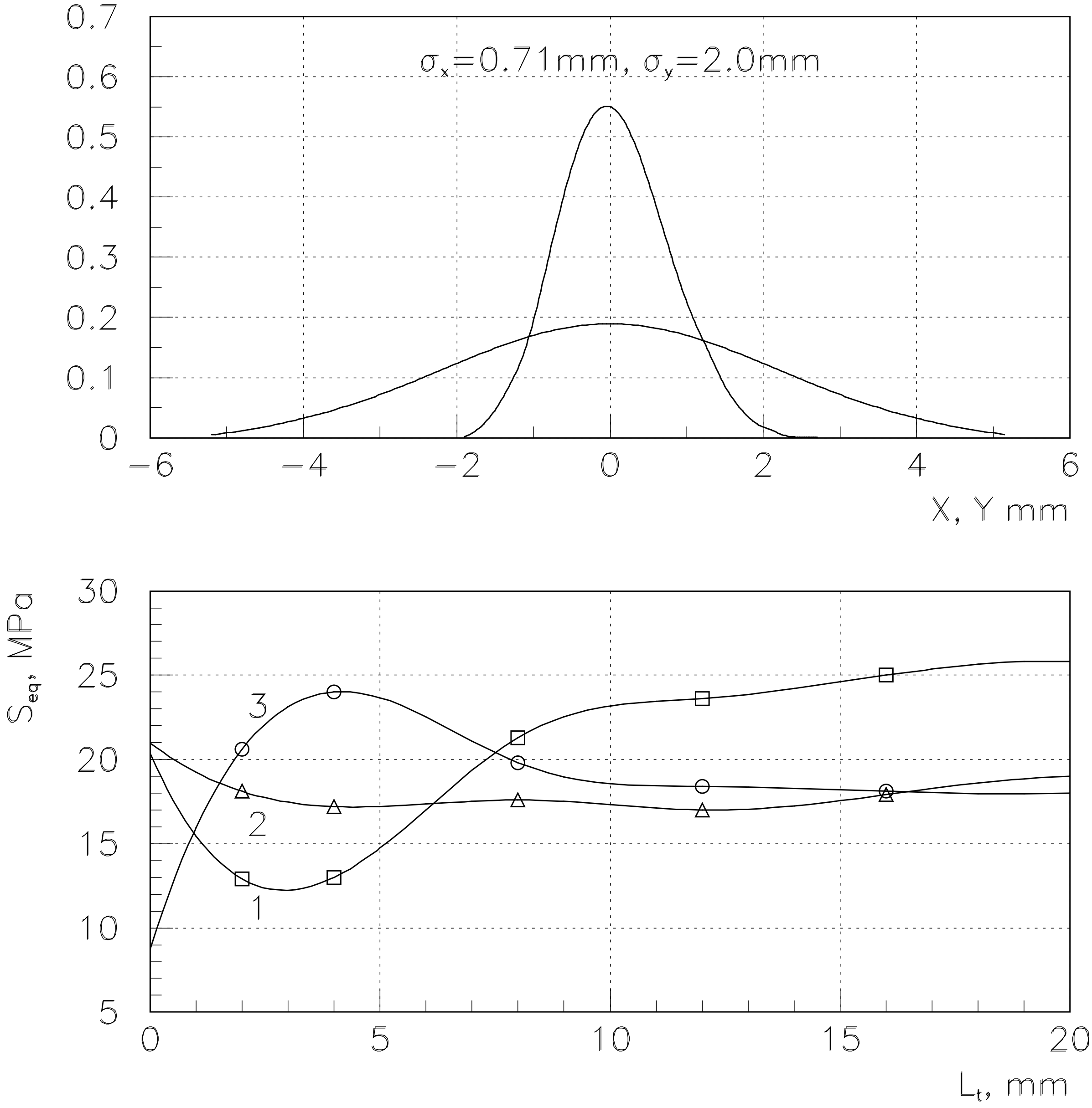

Figure 1.3: Normalized transversal beam distributions in the graphite target and equivalent stresses in most critical points as functions of the tooth length: 1 – point (0,0,0); 2 – point $(+d/2,0,0)$; 3 – point $(0,0,\pm L_t/2)$. Beam intensity is equal to $6{\cdot}10^{13}$ p/spill.

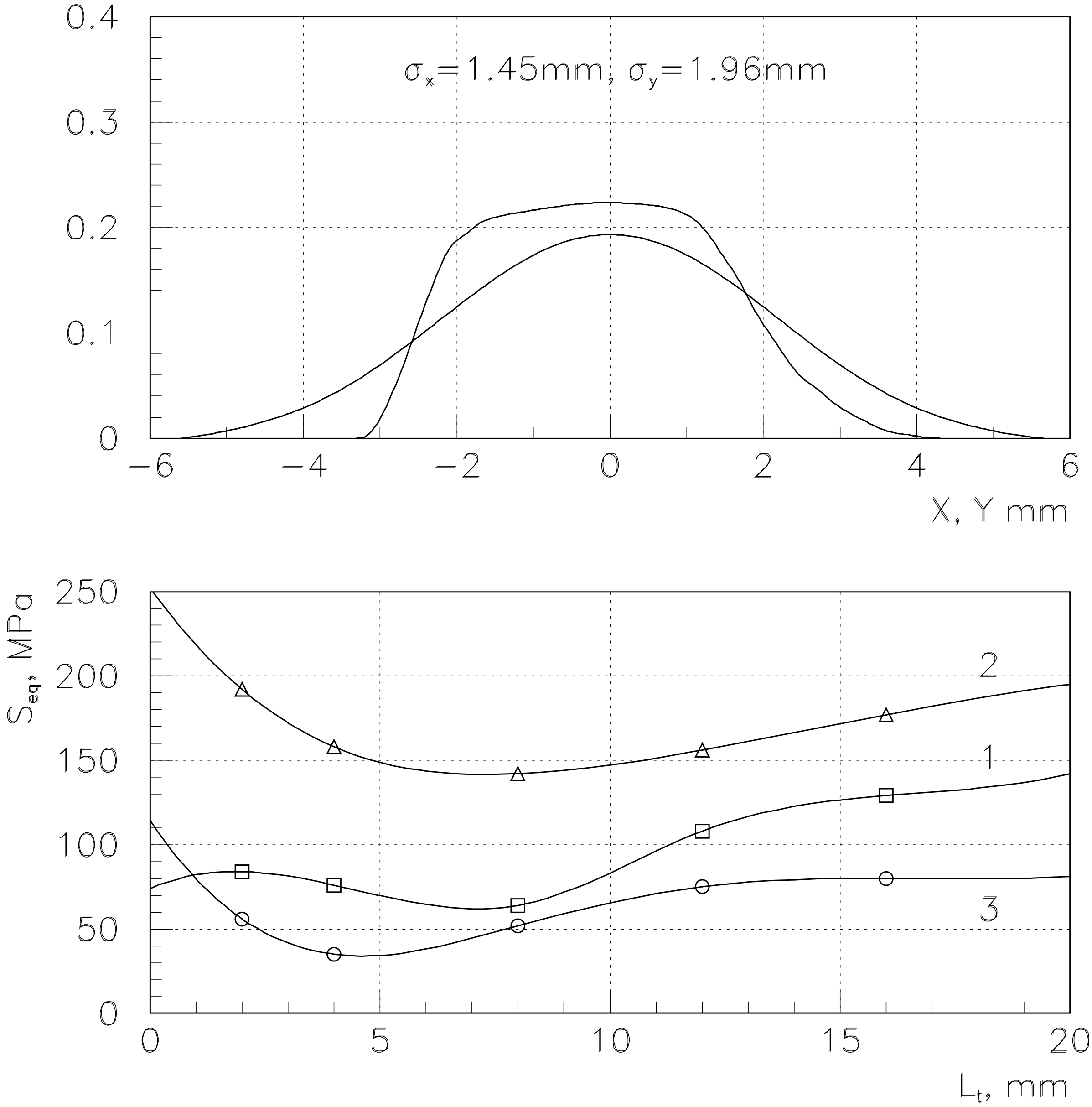

Figure 1.4: Normalized transversal beam distributions in the beryllium target and equivalent stresses in most critical points as functions of the tooth length: 1 – point (0,0,0); 2 – point ($+d/2$,0,0); 3 – point (0,0,$\pm L_t/2$). Beam intensity is equal to $6{\cdot}10^{13}$ p/spill.

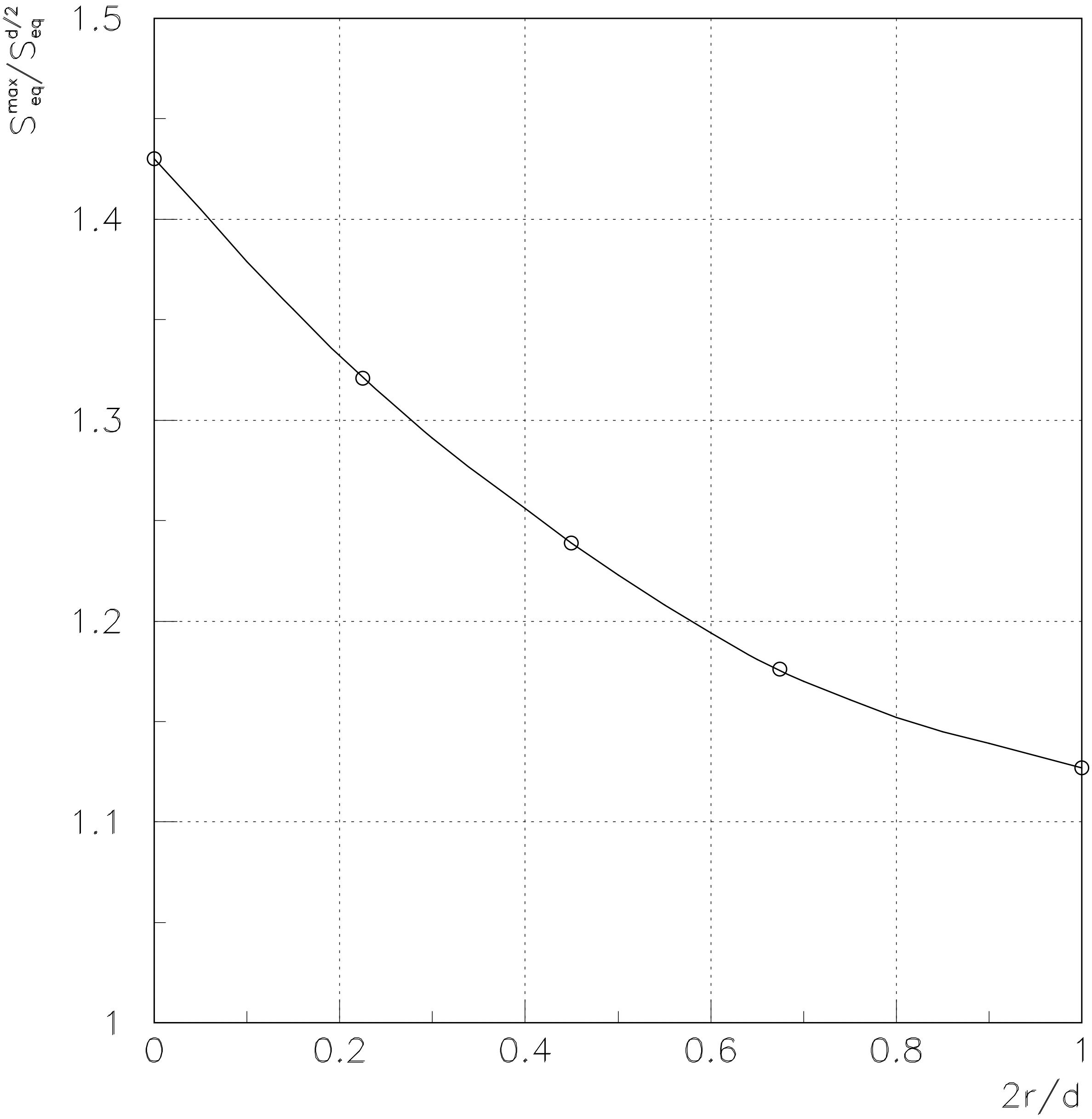

Figure 2.1: The ratio of maximum equivalent stress at the rounded surface to the equivalent stress in the point $(+d/2,0,0)$ as function of rounding radius (d is a thickness of the target piece).

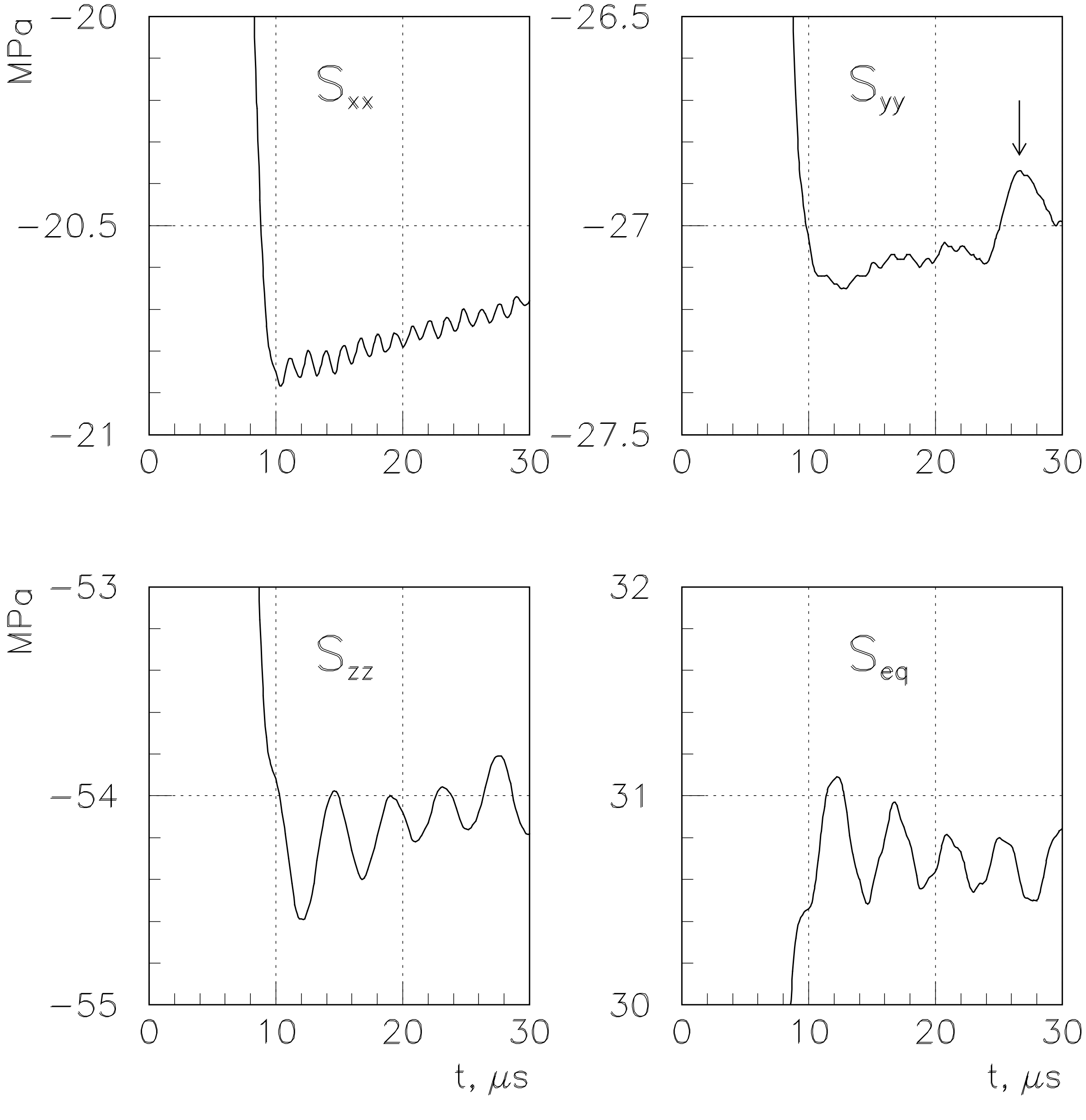

Figure 2.2: Varying in time of stresses in the target tooth.